NHS

Cancer Screening Programmes

Technical evaluation of the

IMS Giotto 3DL Digital Breast Imaging System

TECHNICAL EVALUATION OF THE IMS GIOTTO 3DL DIGITAL BREAST IMAGING SYSTEM

NHSBSP EQUIPMENT REPORT 1301

13 March 2013

Authors

C J Strudley
K C Young
J M Oduko
National Coordinating Centre for the Physics of Mammography

Editor

Kiera Chapman
NHS Cancer Screening Programmes

Typesetting and Design

Mary Greatorex
NHS Cancer Screening Programmes

Document Information	
Title	Technical Evaluation of the IMS Giotto 3DL Digital Breast Imaging System
Policy/document type	NHSBSP Equipment Report
Electronic publication date	March 2013
Version	1
Superseded publications	None
Review date	None
Author/s	C J Strudley, K C Young, J M Oduko
Owner	May be sent to Professor Ken Young, ken.young@nhs.net in readiness for review.
Document objective (clinical/healthcare/social questions covered)	Produced on behalf of the NHSBSP to provide an evaluation of the IMS Giotto 3DL Digital Breast Imaging System.
Population affected	Women eligible for routine and higher-risk breast screening
Target audience	Physicists
Archived	Current document

CONTENTS

ACKNOWLEDGEMENTS

EXECUTIVE SUMMARY

The purpose of this technical evaluation was to determine whether the IMS Giotto 3DL system meets the standards required by the NHS Breast Screening Program, and to provide performance data for comparison against other products. Additional measurements were also undertaken to assess whether the exposure parameters used were optimal.

The system exceeded the minimum acceptable standard for image quality in terms of contrast to noise ratio (CNR) across all simulated breast thicknesses, and the threshold gold detail detection results, obtained using the CDMAM test object, show image quality approaching the achievable level, except for the 0.1 mm details, at the dose levels achieved under automatic exposure control (AEC) for a 60 mm equivalent breast thickness. A 26% increase in image dose for an equivalent breast thickness of 60 mm would be needed to meet the achievable level of image quality for the 0.1 mm details. Adjustment of the doses under AEC control could enable the achievable level to be met for all thicknesses, whilst remaining within the dose limits.

Clinical evaluations are published separately by the NHSBSP for systems that meet the minimum standards in the NHSBSP protocol. A final decision on the suitability of systems for use in the NHSBSP depends on a review of both the technical and clinical evaluations.

1. INTRODUCTION

1.1 Testing procedures and performance standards for digital mammography

This report is one of a series evaluating commercially available digital mammography systems on behalf of the NHS Breast Screening Programme (NHSBSP). The testing methods and standards applied are mainly derived from NHSBSP Equipment Report 0604,[1] and are referred to in this document as 'the NHSBSP protocol'. The standards for image quality and dose within the NHSBSP protocol are the same as those of the European protocol,[2,3] but the latter has been followed where it provides a more detailed performance standard: for example, for the automatic exposure control (AEC) system.

1.2 Objectives

The purpose of these tests was to determine whether this system meets the main standards outlined in the NHSBSP and European protocols, and to provide performance data for comparison against other products. Additional measurements were also undertaken to assess whether the exposure parameters used were optimal.

Clinical evaluations are published separately by the NHSBSP for systems that meet the minimum standards in the NHSBSP protocol. A final decision on the suitability of systems for use in the NHSBSP depends on a review of both the technical and clinical evaluations.

2. METHODS

2.1 System tested

The tests were conducted at the IMS factory in Bologna, Italy on the system shown in Figure 1 and described in Table 1. The amorphous selenium detector is manufactured by Anrad.

Figure 1 Photograph of Giotto 3DL

Table 1   System Description

Manufacturer	IMS
Model	Giotto Image 3DL
System serial number	20-02-32
X-ray tube	IAE XM1016T
Target material	Tungsten
Added filtration	50 µm Rhodium
	50 µm Silver
Detector type	Amorphous selenium
Detector serial number	Detector ID: 2AY93010MA
Pixel size	85 µm (in detector plane)
Detector area	229 x 292 mm
Pixel array	2816 x 3584
Pixel value offset	0
Source to detector distance	650 mm
Source to table distance	620 mm
AEC modes*	Auto
AEC pre-exposure pulse	Varies with compressed breast thickness – see Table 1 below
Software version	Software Versions(s): Raffaello 1.5.4.0 - IMSProc 2.3.1.10

*Auto AEC mode selects kV and filter based on the compressed breast thickness. A pre-exposure pulse is used to calculate the mAs. The pre-pulse contributes to the patient dose but does not contribute to the formation of the image.

2.2   Output and half-value-layer (HVL)

The output and HVL were measured as described in the NHSBSP protocol, at intervals of 3 kV for each target/filter combination.

2.3   Detector response

The detector response was measured as described in the NHSBSP protocol, with a 45 mm thickness of Perspex (polymethylmethacrylate, or PMMA) placed at the tube exit port. An ion chamber was positioned above the table to determine the incident air kerma at the detector surface for a range of manually set mAs values at 29 kV with the W/Ag target/filter combination. The readings were corrected to the surface of the detector using the inverse square law. No correction was made for attenuation by the table and detector cover. Images were saved as unprocessed files and transferred to another computer for analysis. A 10 mm square region of interest (ROI) was positioned on the midline, 6 cm from the chest wall edge of each image. The average pixel value and the standard deviation of pixel values within that region were measured. The relationship between average pixel values and the detector entrance surface air kerma was then determined.

2.4   Dose measurement

Doses were measured using the X-ray set's automatic exposure control (AEC) to expose a range of thicknesses of PMMA. The paddle height was adjusted to leave a gap so that the indicated thickness was equal to the equivalent breast thickness. The dose calculation was carried out using the method and factors in Dance et al[4].

2.5   Contrast to noise ratio (CNR)

To measure the contrast-to-noise ratio (CNR) an aluminium square, 10 mm x 10 mm and 0.2 mm thick, was placed on top of a 10 mm thick block, with one edge on the midline, 6 cm from the chest wall edge. Additional layers of PMMA were placed on top and the paddle height adjusted to simulate a range of breast thicknesses as for the dose measurements (see section 2.4). Twenty small square ROIs (approximately 2.5 mm x 2.5 mm) were used to determine both the average signal and the standard deviation in the signal within the image of the aluminium square (4 ROI) and in the surrounding background area (16 ROI), as shown in Figure 2. Small ROI are used to minimise distortions due to the heel effect and other causes of non-uniformity.[5] This is less important for DR systems than for computed radiography systems, however, because a flat-field correction is applied. The CNR was calculated for each image, as defined in the NHSBSP and European protocols.
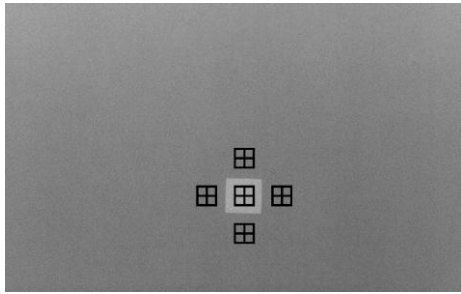
Figure 2   Location and size of ROI used to determine the CNR

To apply the standards in the European protocol, the limiting value for CNR (using 50 mm PMMA) was determined according to Equation 1, below. This equation determines the CNR value ($CNR_{limiting\ value}$) that is necessary to achieve the minimum threshold gold thickness for the 0.1 mm detail (i.e. *threshold gold$_{limiting\ value}$* = 1.68 µm which is equivalent to *threshold contrast$_{limiting\ value}$* = 23.0% using 28 kV Mo/Mo). Threshold contrasts were calculated as described in the European protocol and used in Equation 1.

$$CNR_{limiting\ value} = CNR_{measured} \times \frac{TC_{measured}}{TC_{limiting\ value}} \qquad (1)$$

The relative CNR was then calculated according to Equation 2, and compared with the limiting values provided for relative CNR shown in Table 2. The minimum CNR required to meet this criterion was then calculated.

$$Relative\ CNR = CNR_{measured} / CNR_{limiting\ value} \qquad (2)$$

Table 2   Limiting values for relative CNR

Thickness of PMMA (mm)	Equivalent breast thickness (mm)	Limiting values for relative CNR (%) in European protocol
20	21	>115
30	32	>110
40	45	>105
45	53	>103
50	60	>100
60	75	>95
70	90	>90

2.6   AEC performance for local dense areas

The method used in the European type testing protocol was followed. To simulate local dense areas, a number of images were acquired under AEC control with different thicknesses (2-20 mm) of PMMA providing extra attenuation, as shown in Figure 3.
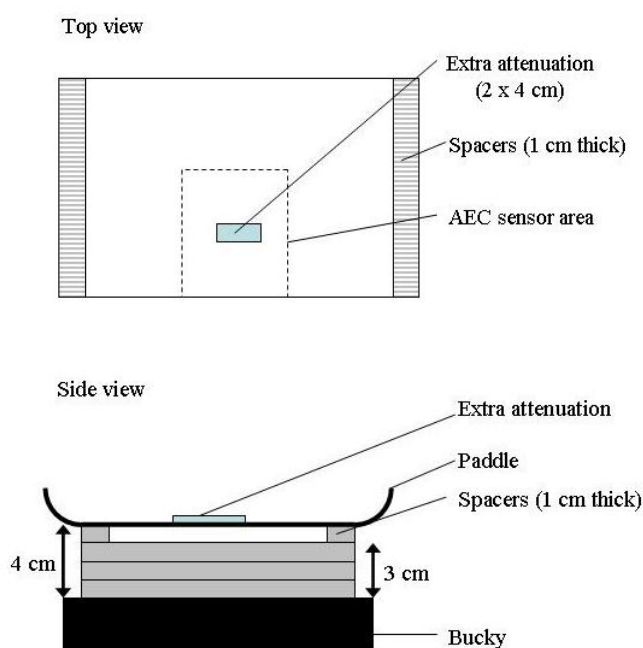
Figure 3   Setup to measure AEC performance for local dense areas

In the area of extra attenuation (20 x 40 mm PMMA), the mean pixel value and standard deviation were measured for a ROI with dimensions 2.5 mm x 2.5 mm, and the signal-to-noise ratio (SNR) calculated.

2.7   Noise analysis

The images acquired for the measurement of detector response using 29 kV W/Ag, were used to analyse the image noise. A ROI with an area of approximately 5 mm x 5 mm was placed on the midline, 4 cm from the chest wall edge. The standard deviation of the pixel values in the ROI for each image was used to investigate the relationship between dose, detector, and image noise. It was assumed that this noise

comprises three components: electronic noise, structural noise, and quantum noise, with the relationship shown in Equation 3:

$$\sigma_p = \sqrt{k_e^2 + k_q^2 p + k_s^2 p^2}$$
(3)

where σ_p is the standard deviation in pixel values within an ROI with a uniform exposure and a mean pixel value p, and k_e, k_q and k_s are the coefficients determining the amount of electronic, quantum, and structural noise. This method of analysis has been described previously[6.] For simplicity, the noise is generally presented here as relative noise defined as in Equation 4.

$$Relative\ noise = \frac{\sigma_p}{p}$$
(4)

The variation in relative noise with mean pixel value was evaluated and fitted using Equation 3, and non-linear regression used to determine the best fit for the constants and their asymptotic confidence limits (using Graphpad Prism Version 5 for Windows[*]). This established whether the experimental measurements of the noise fitted this equation, and the relative proportions of the different noise components. Alternatively, the relationship between noise and pixel values can be approximated by a simple power relationship, as shown in Equation 5.

$$\frac{\sigma_p}{p} = k_t p^{-n}$$
(5)

where k_t is a constant. If the noise were purely quantum noise, the value of n would be 0.5. However the presence of electronic and structural noise means that n can be slightly higher or lower than 0.5.

The variance in pixel values within a ROI is defined as the standard deviation squared. Using the calculated constants, the structural, electronic, and quantum components of the variance were estimated, assuming that each component is independently related to incident air kerma. The percentage of the total variance represented by each component was then calculated and plotted against incident air kerma at the detector. From this, the dose range over which the quantum component dominates can be estimated.

2.8   Image quality measurements

Contrast detail measurements were made using the CDMAM phantom (version 3.4, serial number 1022)[†]. The phantom was positioned with a 20 mm thickness of PMMA above and below, to give a total attenuation approximately equivalent to 50 mm of PMMA or 60 mm of typical breast tissue. The kV target/filter combination and mAs were chosen to match as closely as possible those selected by the AEC when imaging a 5 cm thickness of PMMA. This procedure was repeated to obtain a representative sample of 16 images at this dose level. Unprocessed images were transferred to disk for subsequent analysis offsite. Further images of the test phantom were then obtained at other dose levels by manually selecting higher and lower mAs values with the same beam quality.

---

[*] Graphpad software, San Diego, California, USA, www.graphpad.com.
[†] UMC St. Radboud, Nijmegen University, Netherlands.

An automatic method of reading the CDMAM images was used (CDMAM Analysis UK version 1.4 with CDCOM version 1.6).[7-9] The threshold gold thickness for a typical human observer was predicted using Equation 6.

$$TC_{predicted} = r \, TC_{auto} \tag{6}$$

where $TC_{predicted}$ is the predicted threshold contrast for a typical observer, and TC_{auto} is the threshold contrast measured using an automated procedure with CDMAM images. Contrasts were calculated from gold thickness for a nominal tube voltage of 28 kV and a Mo/Mo target/filter combination as described in the European protocol; r is the average ratio between human and automatic threshold contrast, determined experimentally with the values shown in Table 3.[7]

Table 3   Values of r used to predict threshold contrast

Diameter of gold disc (mm)	Average ratio of human to automatically measured threshold contrast (r)
0.08	1.40
0.10	1.50
0.13	1.60
0.16	1.68
0.20	1.75
0.25	1.82
0.31	1.88
0.40	1.94
0.50	1.98
0.63	2.01
0.80	2.06
1.00	2.11

The main advantage of automatic reading is that it has the potential to eliminate observer error, which is a significant problem when using human observers. However it should be noted that, at the present time, the official protocols are based on human reading.

The predicted threshold gold thickness for each detail diameter at each dose level was fitted with a curve, as described in the NHSBSP protocol. The confidence limits for the predicted threshold gold thicknesses have been previously determined using a resampling method with a large set of images.

The expected relationship between threshold contrast and dose is shown in Equation 7.

$$Threshold \; contrast \; = \; \lambda \, D^{-n} \tag{7}$$

where D represents the mean glandular dose (MGD) calculated for a 60 mm standard breast equivalent to the test phantom configuration used for the image quality measurement, and λ is a constant to be fitted. It is assumed that a similar equation applies when using threshold gold thickness instead of contrast. This equation was plotted with the experimental data for each detail size from 0.1 mm to 1.0 mm. The value of n resulting in the best fit to the experimental data was determined.

2.9   Image retention

Image retention was measured as described in the NHSBSP protocol using Equation 8. The regions used are shown in Figure 4.
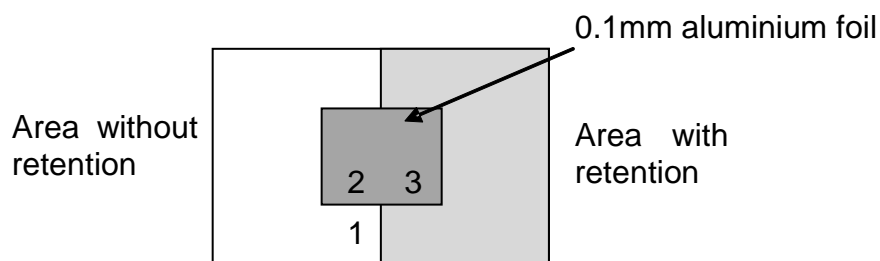
Figure 4   Position of ROI used for calculation of the image retention factor

$$Image\ retention\ factor = \frac{mean\ pixel\ value\,(region\ 3) - mean\ pixel\ value\,(region\ 2)}{mean\ pixel\ value\,(region\ 1) - mean\ pixel\ value\,(region\ 2)} \tag{8}$$

2.9   Physical measurements of the detector performance

The modulation transfer function (MTF), normalised noise power spectrum (NNPS), and detective quantum efficiency (DQE) of the detector were measured. The methods used were as close as possible to those described by the International Electrotechnical Commission (IEC).[10] The radiation quality used for the measurements was adjusted by placing an aluminium filter of a uniform 2 mm thickness at the tube housing. The beam quality used was 28 kV W/Ag. The test device to measure the MTF comprised a 0.8 mm thick rectangle (120 mm x 60 mm) of stainless steel with polished straight edges. This test device was placed on top of the detector with the grid removed and positioned to measure the MTF in two directions, first perpendicular, and then parallel to the chest wall edge. To measure the noise power spectrum, the test device was removed and exposures made for a range of incident air kermas at the surface of the detector. The DQE is presented as the average of the results for directions parallel and perpendicular to the chest wall edge.

2.10   Optimisation

A method for determining optimal beam qualities and exposure factors for digital mammography systems has been described previously and was used to evaluate this system.[6,11] CNR and mean glandular dose were measured as described above, using 20 to 70 mm thick blocks of PMMA. For each thickness, four tube voltage settings were used (25, 28, 31, and 34 kV) with each of the target/filter combinations available and the mAs recorded. The MGDs to typical breasts with attenuation equivalent to each thickness of the PMMA were calculated, as described in the NHSBSP protocol. Equation 9 was used to calculate the dose required to achieve a target CNR:

$$CNR = k\,D^{-n} \tag{9}$$

where *k* is a constant to be fitted, *D* is the MGD for a breast of equivalent thickness, and n is the value already found by fitting Equation 5 to the noise analysis data.

The target CNR was that calculated to reach either the minimum or achievable image quality as specified in the NHSBSP and European protocols using the following relationship:

$$Threshold\ contrast = \frac{\lambda}{CNR} \tag{10}$$

where λ is a constant that is independent of dose, beam quality, and the thickness of attenuating material. The optimal beam quality for each thickness was selected as that necessary to achieve the target CNR for the minimum dose.

3. RESULTS

3.1 Output and HVL

The results are shown in Table 4.

Table 4   Output and HVL

kV Target/ Filter	Output (μGy/mAs at 1 m)	HVL (mm Al)	kV Target/ Filter	Output (μGy/mAs at 1 m)	HVL (mm Al)
25 W/Rh	13.9	0.48	25 W/Ag	15.4	0.50
28 W/Rh	18.9	0.52	28 W/Ag	22.0	0.55
31 W/Rh	24.1	0.54	31 W/Ag	28.6	0.59
34 W/Rh	29.4	0.56	34 W/Ag	35.4	0.62

3.2 Detector response

The detector was found to have a linear response, with a zero offset, as shown in Figure 5.
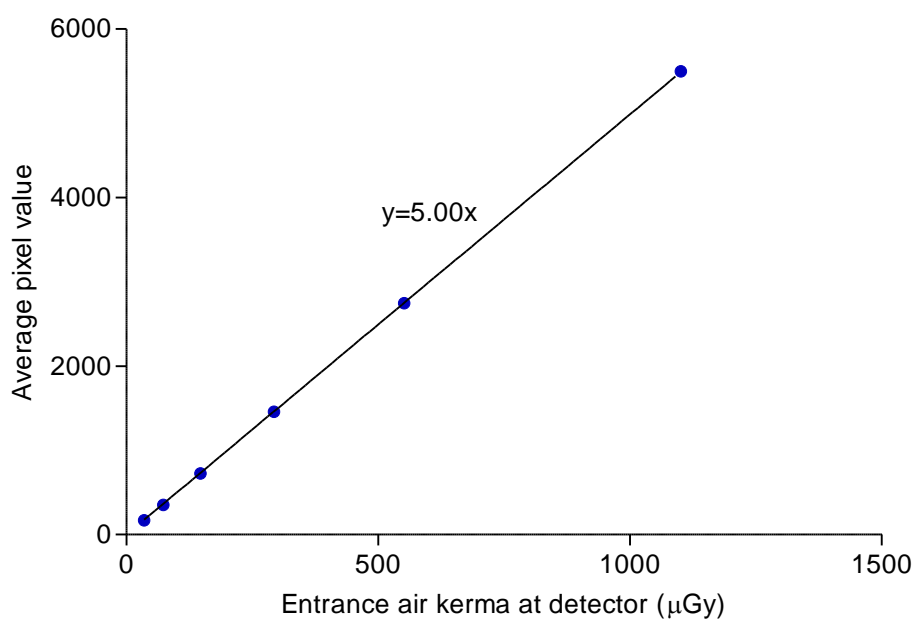
Figure 5   Detector response

3.3   AEC performance

3.3.1   Dose

The MGD for breasts simulated with PMMA exposed under AEC control are shown in Table 5 and Figure 6. At all thicknesses, the dose was below the remedial level specified in the NHSBSP protocol, which is the same as the maximum acceptable level in the European Protocol.

The pre-exposure pulse used in AEC modes ranged from 4 mAs to 22 mAs, depending on indicated compressed breast thickness. This exposure contributes to the MGD, but is not used to produce the digital image. It is understood that the manufacturer has since reduced the pre-exposure pulse in subsequent AEC software versions.

Table 5   Mean glandular dose for simulated breasts (Auto AEC mode)

PMMA thickness (mm)	Equivalent breast thickness (mm)	kV	Target	Filter	Pre-exposure mAs**	Total mAs*	MGD (mGy)	NHSBSP remedial level (mGy)
20	21	24	W	Rh	4	41	0.66	> 1.0
30	32	25	W	Ag	5	54	0.91	> 1.5
40	45	27	W	Ag	8	58	1.11	> 2.0
45	53	29	W	Ag	10	58	1.31	> 2.5
50	60	30	W	Ag	12	65	1.56	> 3.0
60	75	31	W	Ag	19	101	2.37	> 4.5
70	90	33	W	Ag	22	127	3.14	> 6.5

*The total mAs includes the pre-exposure mAs.
**Values for pre-exposure mAs supplied by the manufacturer.
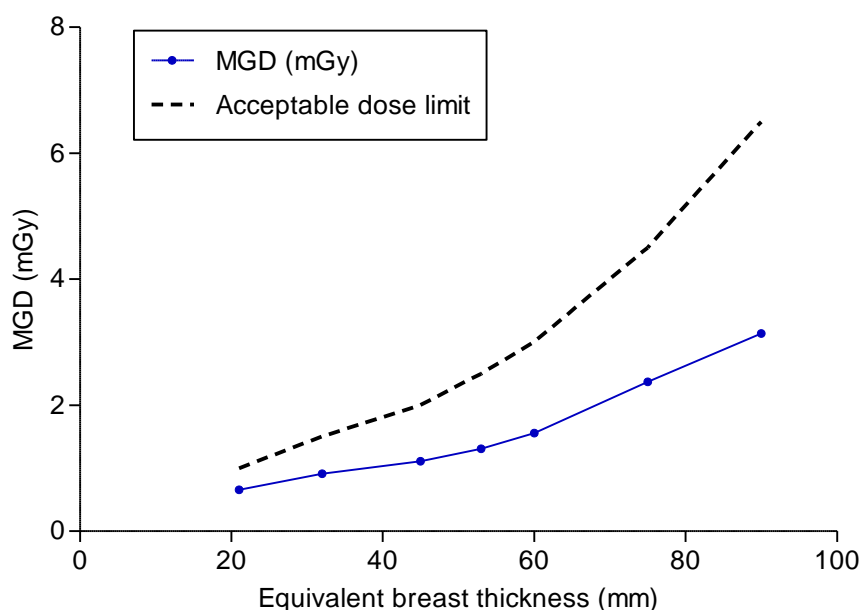
Figure 6   MGD for different thicknesses of simulated breasts using the Auto AEC mode

3.3.2   CNR

The results of the contrast and CNR measurements are shown in Table 6 and Figure 7. The CNR required to meet the minimum acceptable and achievable image quality standards at the 60 mm breast thickness have been calculated and are also shown in Table 6 and Figure 7. The CNR required at each thickness to meet the limiting values for CNR in the European protocol are also shown. The background pixel values in the CNR images increased with increasing breast thickness. These pixel values approximate to incident air kermas at the detector in the range 80 to 140 µGy, as determined by comparison with data in Figure 5.

Table 6   Contrast and CNR measurements using AEC

Equivalent breast thickness (mm)	kV Target/ Filter	mA s*	Back-ground pixel value	% contrast for 0.2 mm Al	Measured CNR	CNR at mini-mum accept-able IQ	CNR at achiev-able IQ	CNR to meet Euro. limiting value	European limiting values for relative CNR
21	24 W/Rh	37	395	15.9%	10.9	5.8	8.8	6.7	>115%
32	25 W/Ag	49	477	13.1%	9.7	5.8	8.8	6.4	>110%
45	27 W/Ag	50	474	11.3%	8.2	5.8	8.8	6.1	>105%
53	29 W/Ag	48	507	10.6%	7.9	5.8	8.8	6.0	>103%
60	30 W/Ag	53	527	9.8%	7.3	5.8	8.8	5.8	>100%
75	31 W/Ag	82	591	9.0%	7.1	5.8	8.8	5.5	>95%
90	33 W/Ag	105	677	7.8%	6.2	5.8	8.8	5.2	>90%

*mAs values here do not include pre-exposure mAs as this does not contribute to the image
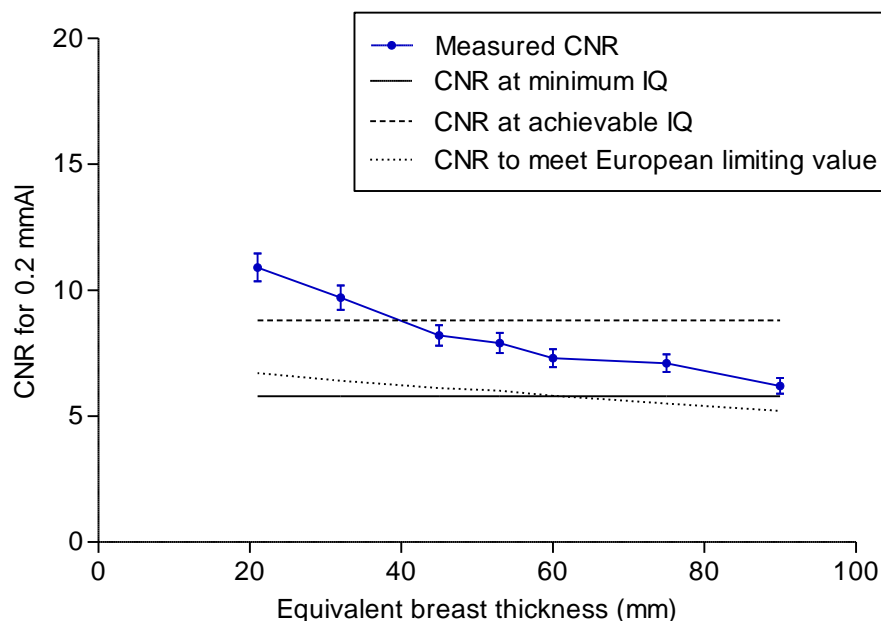
Figure 7   Measured CNR compared with the limiting values in the European protocol for the system (Error bars indicate 95% confidence limits.)

3.3.3 AEC performance for local dense areas

It is expected that when the AEC adjusts for locally dense areas, the SNR will remain constant as additional attenuation (PMMA) is added within the simulated local dense area. The results presented in Table 7 and Figure 8 show that the AEC behaves as expected, with the SNR over the increasing local dense area remaining fairly constant as the tube load increases.

Table 7   AEC performance for local dense areas (Auto mode)

Attenuation (mm PMMA)	Target /Filter	Tube voltage (kV)	Tube load (mAs)	SNR
30	W/Ag	26	42	71.9
32	W/Ag	26	44	69.6
34	W/Ag	26	49	71.5
36	W/Ag	26	54	70.1
38	W/Ag	26	59	69.2
40	W/Ag	26	65	69.2
42	W/Ag	26	70	69.0
44	W/Ag	26	77	68.2
46	W/Ag	26	85	74.5
48	W/Ag	26	92	68.4
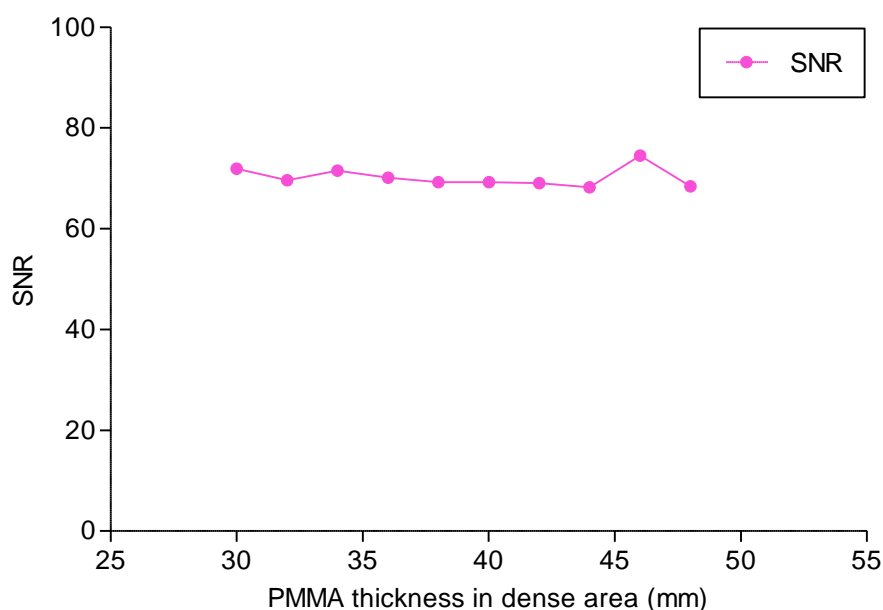
Figure 8   AEC performance for local dense areas

3.4   Noise measurements

The variation in noise with dose was analysed by plotting the standard deviation in pixel values against the detector entrance air kerma, as shown in Figure 9. The fitted power curve has an index of 0.46. If quantum noise sources alone were present, the data would form a straight line with an index of 0.5. The data starts to deviate from a straight line at lower doses due to the presence of electronic noise. This is normal for such systems. Quantum noise was the dominant noise source.
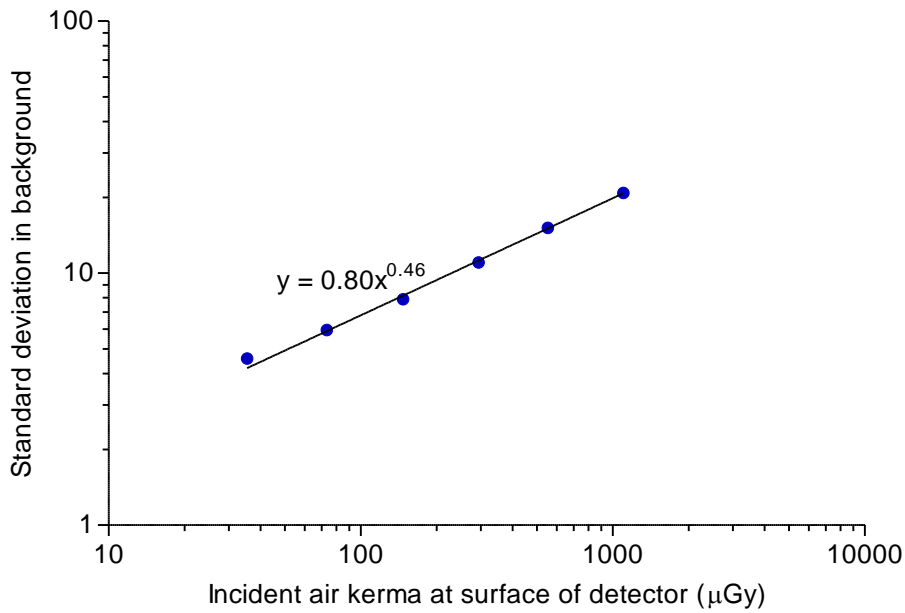
Figure 9   Standard deviation of pixel values versus air kerma at detector

Figure 10 is an alternative way of presenting the data and shows the relative noise at different entrance air kermas. The estimated relative contributions of electronic, structural, and quantum noise are shown and the quadratic sum of these contributions fitted to the measured noise (using Equation 3). Figure 11 shows the different amounts of variance due to each component. Quantum noise predominates over the clinical range.
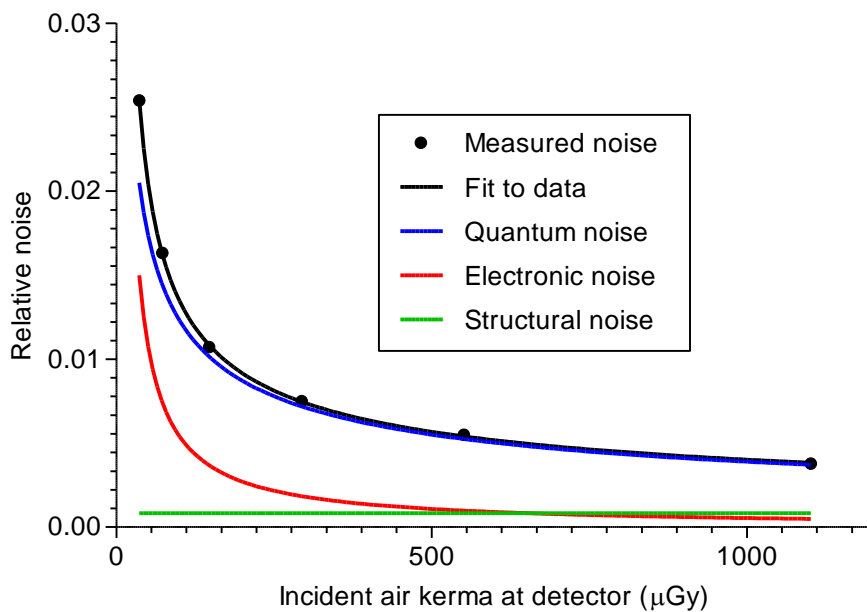
Figure 10   Relative noise and noise components at different pixel values.
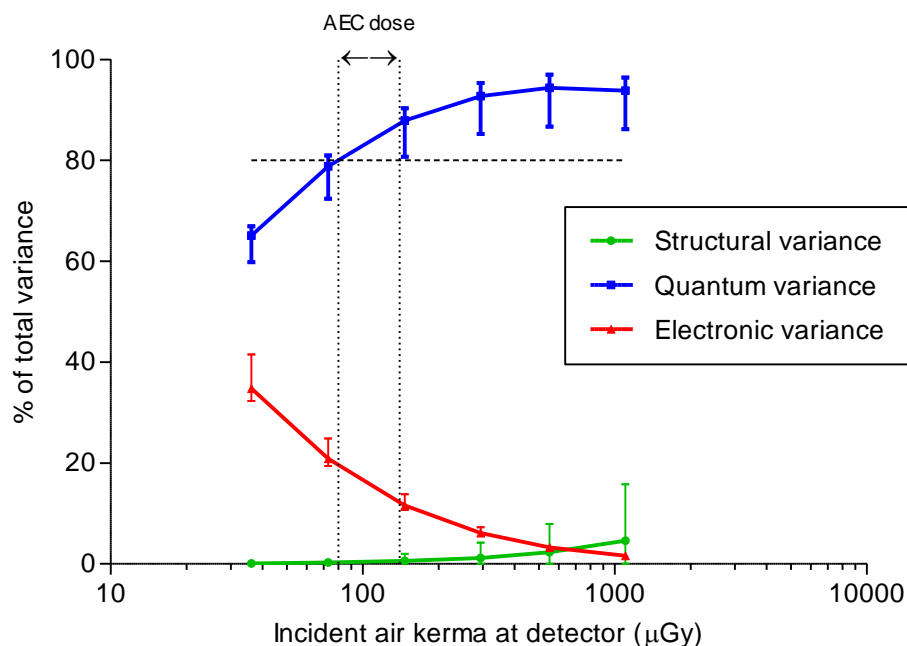
Figure 11 Each noise component as a percentage of the total variance. The percentage quantum variance is compared to a limit of 80%, and the two vertical dotted lines show the range of incident air kermas at the detector obtained under AEC control. Error bars indicate 95% confidence limits.

3.5   Image quality measurements

Exposures of the image quality phantom were made by manual selection of the same beam quality as was selected by the AEC for an equivalent breast (60 mm thick). The mAs was selected to match that which would be used in an image taken under AEC control (excluding the prepulse). This resulted in exposure factors of 30 kV W/Ag, 53 mAs, giving an MGD of 1.27 mGy. Subsequent image quality measurements were made by manual selection, at a range of mAs values between approximately half and three times the AEC-selected mAs, at the same beam quality, as shown in Table 8.

Table 8   Images acquired for image quality measurement

Exposure mode	kV target/ filter	Tube loading (mAs)	MGD to equivalent breasts 60 mm thick (mGy)	Number of CDMAM images acquired and analysed
manual	30 kV W/Ag	31	0.74	16
manual	30 kV W/Ag	44	1.06	16
manual	30 kV W/Ag	53	1.27	16
manual	30 kV W/Ag	95	2.28	16
manual	30 kV W/Ag	158	3.80	16

The contrast detail curves at the different dose levels (determined by automatic reading of the images) are shown in Figure 12. The threshold gold thicknesses for different diameters and the different dose levels are shown in Table 9, along with the minimum and achievable threshold values from the NHSBSP protocol (which are the same as the European protocol).

The measured threshold gold thicknesses are plotted against the MGD for an equivalent breast for the 0.1 and 0.25 mm detail sizes in Figure 13. The curves in Figure 13 were interpolated to find the doses required to meet the minimum acceptable and achievable threshold gold thicknesses.

Table 9   Average threshold gold thicknesses for different detail diameters for five doses using 30 kV W/Ag and automatically predicted data.

| Dia-meter (mm) | Threshold gold thickness (µm) | | | | | | |
	Accept-able value	Achiev-able value	MGD = 0.74 mGy	MGD = 1.06 mGy	MGD = 1.27 mGy	MGD = 2.28 mGy	MGD = 3.8 mGy
0.1	1.680	1.100	1.983 ± 0.137	1.521 ± 0.109	1.340 ± 0.092	0.839 ± 0.060	0.550 ± 0.041
0.25	0.352	0.244	0.362 ± 0.025	0.261 ± 0.018	0.248 ± 0.018	0.204 ± 0.013	0.142 ± 0.010
0.5	0.150	0.103	0.137 ± 0.011	0.114 ± 0.009	0.106 ± 0.008	0.074 ± 0.006	0.061 ± 0.004
1	0.091	0.056	0.084 ± 0.009	0.066 ± 0.008	0.058 ± 0.006	0.040 ± 0.004	0.024 ± 0.003
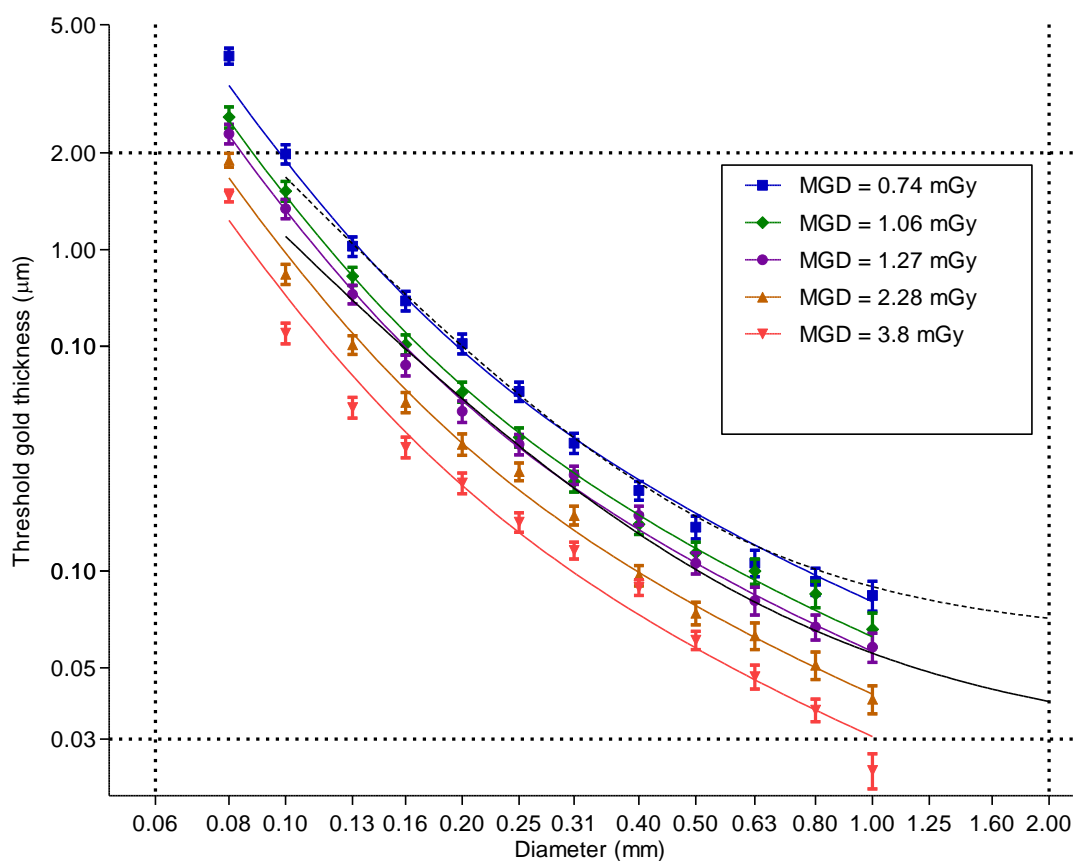
Figure 12 Contrast-detail curves for five doses at 30 kV W/Ag using predicted results from automated reading. The 1.27 mGy dose corresponds to the AEC selection. Error bars indicate 95% confidence limits.
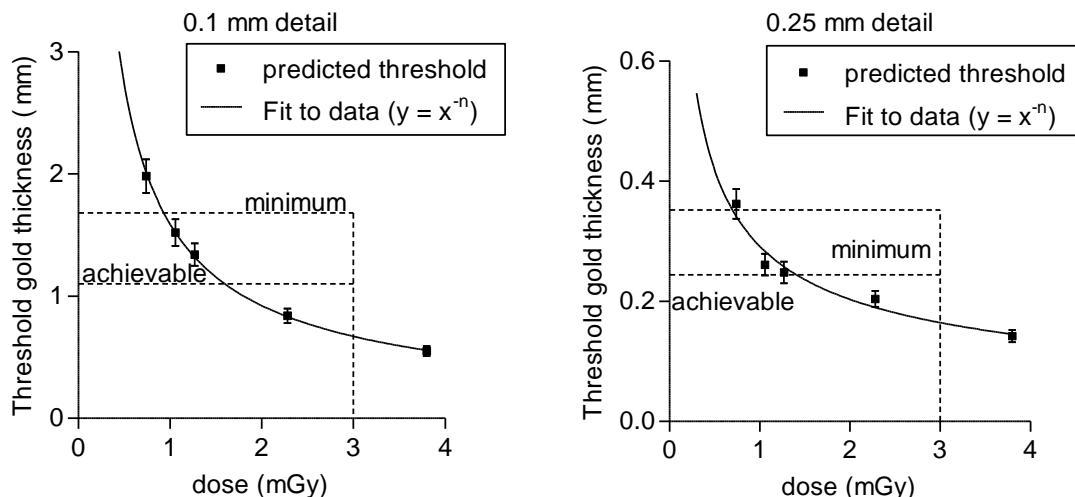
Figure 13 Threshold gold thickness at different doses. The doses are for a breast equivalent to a 5 cm thickness of PMMA. Error bars indicate 95% confidence limits.

3.6   Comparison with other systems

The MGDs to reach the minimum and achievable image quality standards in the NHSBSP protocol have been estimated from the curves shown in Figure 13. (The error in estimating these doses depends on the accuracy of the curve fitting procedure, and pooled data for several systems has been used to estimate the 95% confidence limits of approximately 20%.) These doses are shown against similar data for other models of digital mammography system in Tables 10 and 11 and Figures 14 to 17. The data for the other systems derives from previously published results, determined using the same methods described in this report.[3,12-23] The data for film screens represent an average value, which was determined using a variety of modern film screen systems.

Table 10   The MGD required to reach the minimum threshold gold thickness for 0.1 and 0.25 mm details for different systems

System	MGD (mGy) for 0.1 mm		MGD (mGy) for 0.25 mm	
	Human	Predicted	Human	Predicted
Philips MDM-L30	0.41		0.41	0.42
Siemens Inspiration	0.97	0.76	0.87	0.60
Fuji Amulet	0.62	0.67	0.74	0.71
Hologic Dimensions	0.56	0.38	0.65	0.40
Hologic Selenia (W)	0.58	0.71	0.65	0.64
GE Essential	0.60	0.49	0.50	0.49
GE DS	1.01	0.82	0.87	0.83
IMS Giotto (W)	1.07	1.38	0.91	1.17
IMS Giotto 3DL		0.93		0.70
Film screen	1.17	1.30	1.07	1.36
Agfa CR85-X (NIP)	1.24	1.27	1.06	0.96
Agfa CR (MM3.0)[†]	2.54	2.32	1.45	1.54
Fuji Profect CR	1.67	1.78	1.45	1.35
Carestream CR (EHR-M2)	2.29	2.34	1.45	1.80
Konica Minolta (CP-1M)	1.60	1.47	1.12	0.99

[†]Data are the mean of measurements shown in NHSBSP Equipment Reports 0707[9] and 0905.[15]

Table 11   The MGD required to reach the achievable threshold gold thickness for 0.1 and 0.25 mm details for different systems.

System	MGD (mGy) for 0.1 mm		MGD (mGy) for 0.25 mm	
	Human	Predicted	Human	Predicted
Philips MDM-L30	1.27	1.74	1.37	0.95
Siemens Inspiration	2.06	1.27	1.68	1.16
Fuji Amulet	1.40	1.13	1.50	1.41
Hologic Dimensions	1.29	0.91	1.23	0.85
Hologic Selenia (W)	1.66	1.37	1.61	1.48
GE Essential	1.57	1.13	1.14	1.03
GE DS	2.35	1.57	1.80	1.87
IMS Giotto (W)	2.33	2.73	1.77	2.11
IMS Giotto 3DL		1.60		1.41
Film screen	2.48	3.03	2.19	2.83
Agfa CR85-X (NIP)	3.22	2.47	2.40	2.34
Agfa CR (MM3.0)[†]	5.21	5.14	3.72	3.82
Fuji Profect CR	4.26	3.29	3.52	2.65
Carestream CR (EHR-M2)	5.34	5.45	3.03	3.74
Konica Monolta (CP-1M)	4.53	3.45	2.73	2.08

[†]Data are the mean of measurements shown in NHSBSP Equipment Reports 0707[9] and 0905.[15]
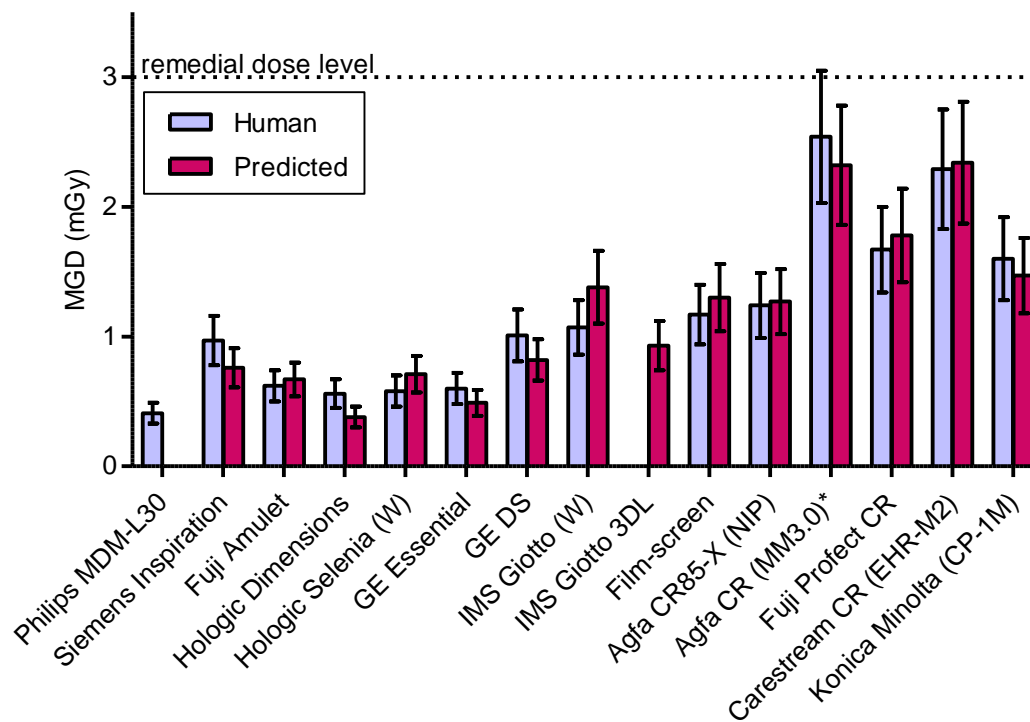
Figure 14 Dose to reach minimum acceptable image quality standard for 0.1 mm detail. Error bars indicate 95% confidence limits.
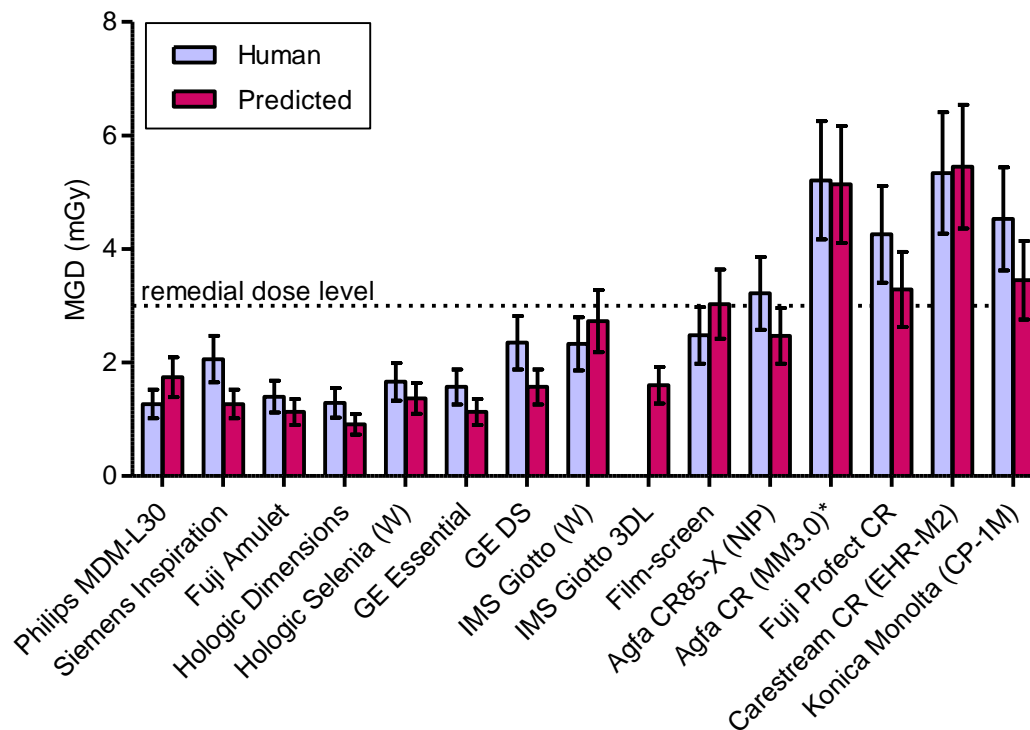
Figure 15 Dose to reach achievable image quality standard for 0.1 mm detail. Error bars indicate 95% confidence limits.
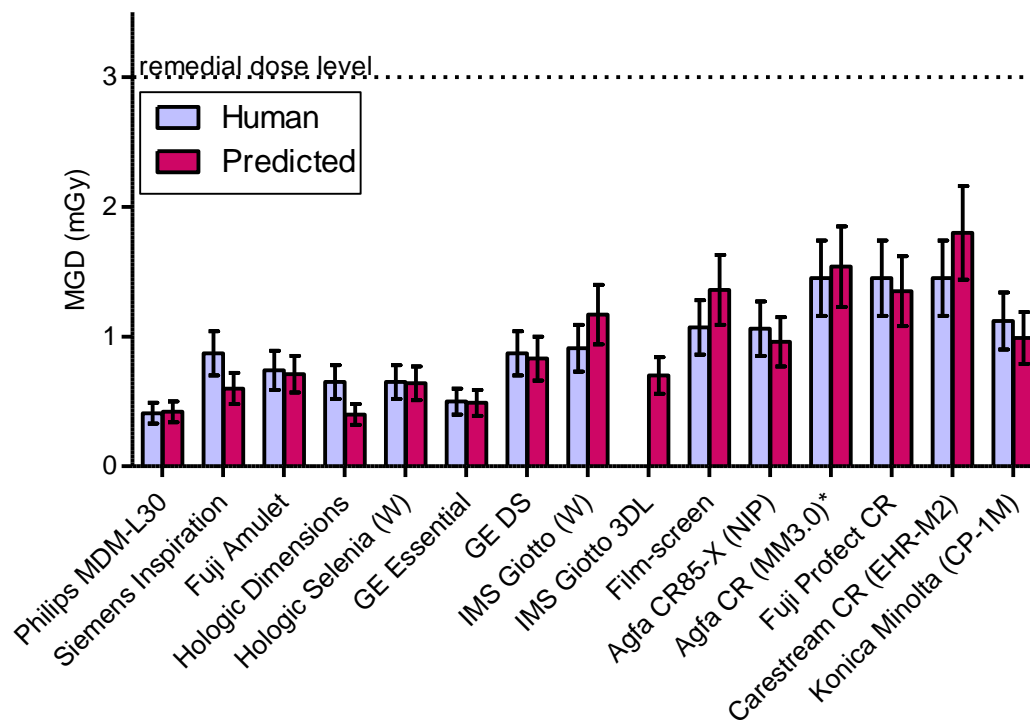
Figure 16 Dose to reach minimum acceptable image quality standard for 0.25 mm detail. Error bars indicate 95% confidence limits.
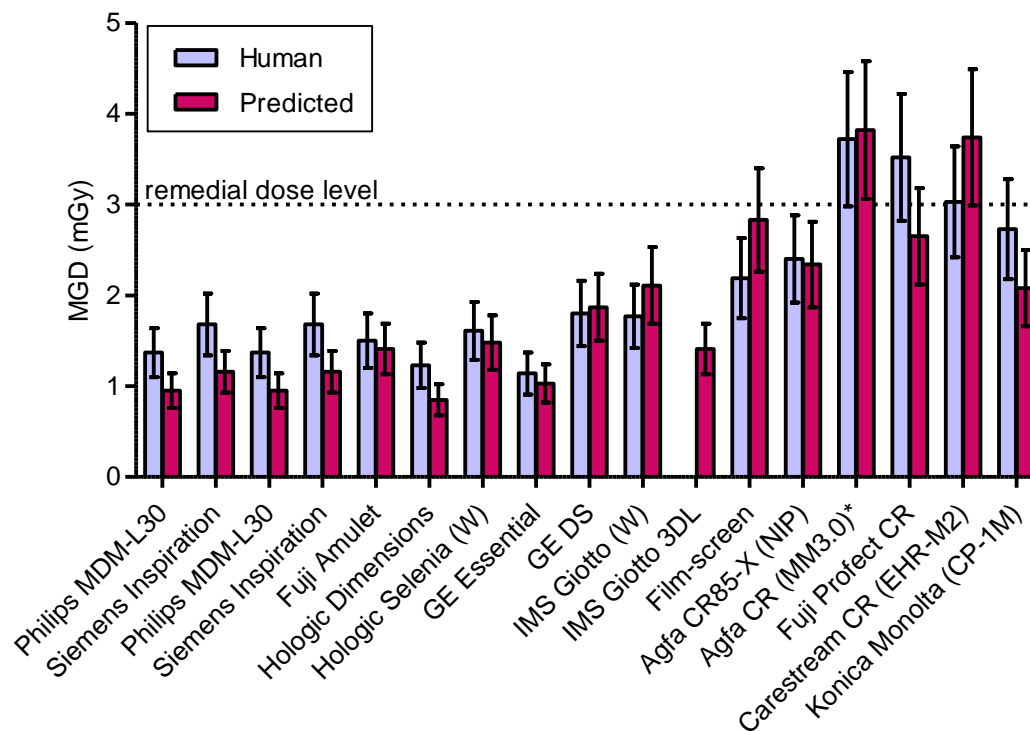
Figure 17 Dose to reach achievable image quality standard for 0.25 mm detail. Error bars indicate 95% confidence limits.

3.7 Image retention

The results are shown in Table 12.

Table 12   Image retention factor

ROI	Pixel value
1	609.3
2	610.4
3	652.2
image retention factor: 0.002	
Limiting value: 0.3	

3.8 Detector performance

The MTF is shown in Figure 18 for the two orthogonal directions. Figure 19 shows the DQE averaged in the two orthogonal directions for a range of entrance surface air kermas (ESAK). The MTF and DQE measurements were interpolated to show values at standard frequencies (Table 13).
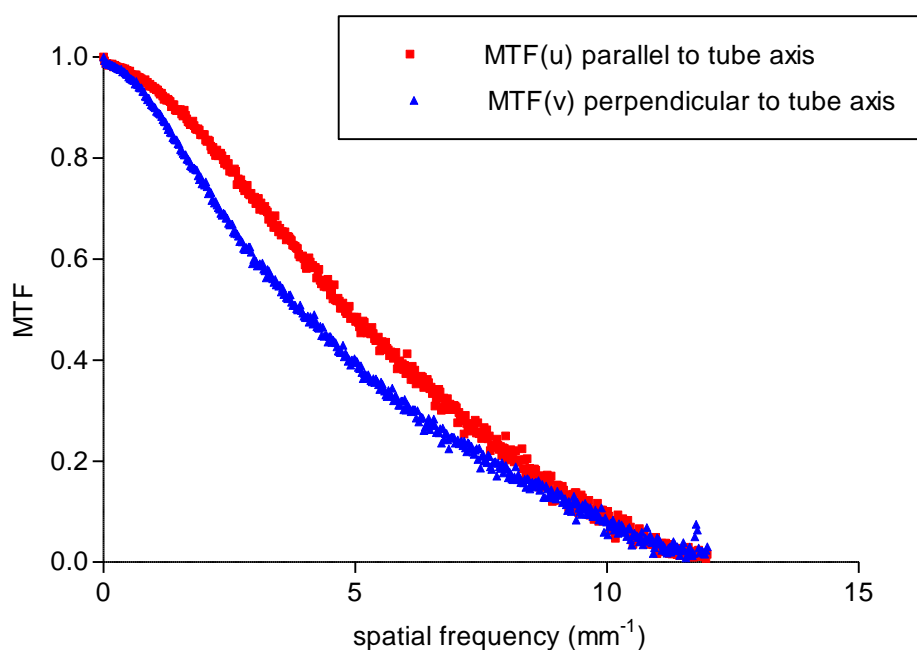
Figure 18   Pre-sampling MTF.
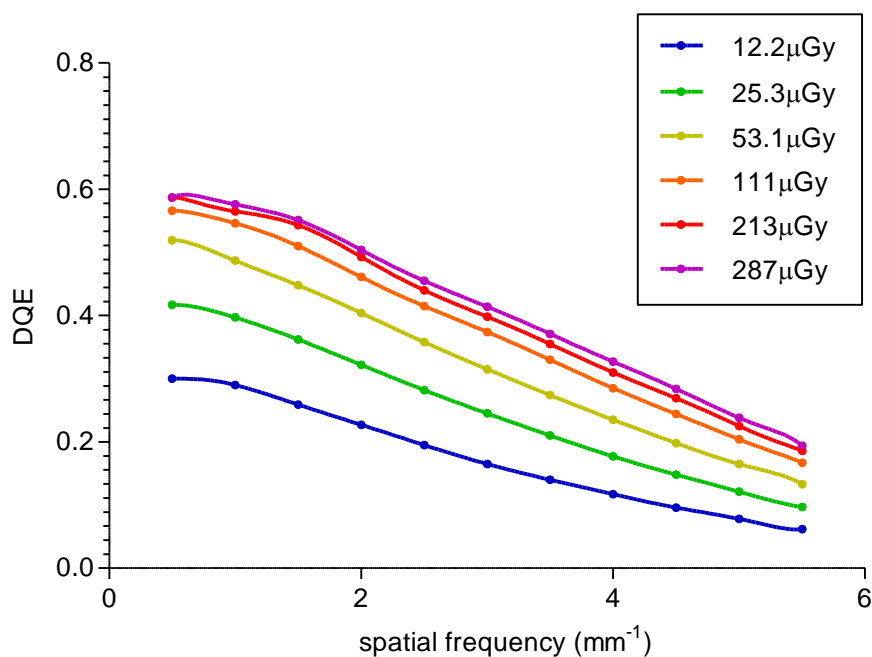
Figure 19 DQE averaged in both directions using 28kV W/Ag and a range of entrance air kermas.

Table 13   MTF and DQE measurements at standard frequencies (DQE at 111µGy).

Frequency (mm^{-1})	MTF (u)	MTF (v)	MTF (uv)	DQE (uv)
0.5	0.97	0.96	0.97	0.57
1.0	0.94	0.90	0.92	0.55
1.5	0.89	0.83	0.86	0.51
2.0	0.84	0.75	0.79	0.46
2.5	0.78	0.67	0.73	0.41
3.0	0.72	0.60	0.66	0.37
3.5	0.66	0.54	0.60	0.33
4.0	0.60	0.49	0.54	0.29
4.5	0.54	0.44	0.49	0.24
5.0	0.48	0.39	0.44	0.20
5.5	0.43	0.35	0.39	0.17

3.9   Optimisation

The target CNR corresponding to the achievable image quality was calculated to be 11.3. The MGD required to reach this target CNR for each beam quality and different thicknesses of PMMA is shown in Figure 20. From these data, the optimal beam qualities were selected and are shown in Table 14. The beam qualities in Table 14 are similar to those chosen by the AEC. In order to reach the achievable level of image quality, the dose would need to be increased by around 40% for the largest breast size, represented by 70 mm PMMA. At this level, the dose would still be well within the dose limit set in the NHSBSP protocol.
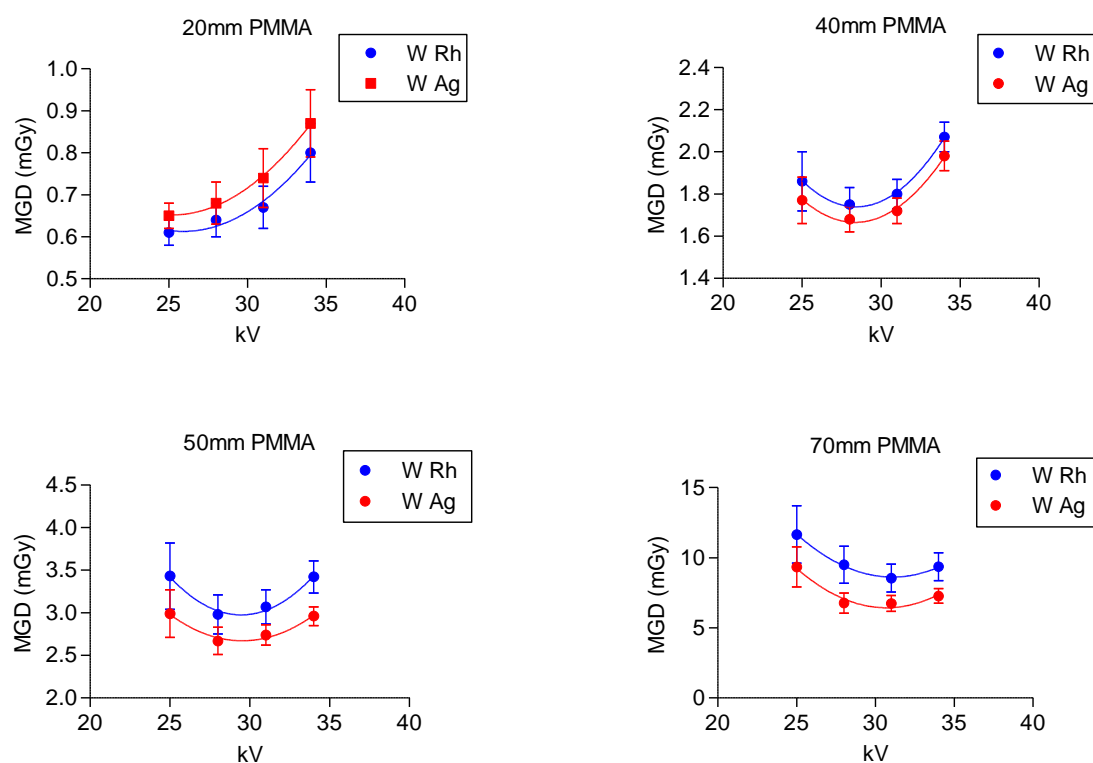
Figure 20 MGD to reach the achievable image quality standard in the NHSBSP protocol (error bars indicate 95% confidence limits)

Table 14   Optimal factors to produce achievable image quality (where CNR = 8.8)

PMMA Thickness	kV target/ filter	Background pixel value	mAs	MGD (mGy)	MGD (mGy) when AEC selected factors used	% change in dose if optimal factors used (cf AEC selection)	Remedial dose level in NHSBSP protocol (mGy)
20	25 W/Rh	279	22	0.40	0.66	-39%	1.0
40	28 W/Ag	560	51	1.11	1.11	0%	2.0
50	28 W/Ag	624	93	1.77	1.56	+13%	3.0
70	31 W/Ag	938	217	4.46	3.14	+42%	6.5

4.   DISCUSSION

The detector response was linear, with no offset. The noise analysis confirmed that quantum noise is the dominant noise source. As with most systems, there was also evidence of some electronic noise. There appeared to be very little structural noise. The AEC resulted in doses to simulated breasts that were well below the limits set in the NHSBSP protocol. The dose for the standard breast simulated with 45 mm of PMMA was 1.31 mGy. At this thickness, an upper limit of 2.5 mGy is set by the NHSBSP.

The AEC settings resulted in background pixel values ranging from approximately 400 for 2 cm of PMMA to 700 for 7 cm of PMMA, corresponding to an incident air kermas ranging from approximately 80 to 140 µGy. Despite the fact that pixel values increased with PMMA thickness, the CNR decreased with increasing PMMA thickness. The target CNR required for minimum acceptable image quality was exceeded across the full range of breast thicknesses, but the achievable level of image quality was only met for the smaller equivalent breast thicknesses (Figure 7).

The AEC test for dense areas showed that as the local dense area increased in attenuation, a constant SNR was maintained within the dense area, which is satisfactory and as expected for a modern AEC.

The image quality measurements indicated that for the standard thickness tested (60 mm equivalent breast) the image quality for this system was close to the achievable level for all but the smallest detail size (0.1 mm diameter) at a dose of 1.27 mGy (using 30 kV W/Ag), which is equal to that selected by the AEC minus the pre-exposure pulse. It is expected that modern digital mammography systems operate at or above the achievable image quality level. An MGD of 1.6 ± 0.3 mGy (excluding the pre-exposure pulse) was calculated to be necessary to reach the achievable image quality level for all detail sizes for this system, compared to the remedial level of 3 mGy at this thickness. It is understood from the manufacturer that the size of the pre-exposure pulse has since been reduced for systems with the latest AEC software.

The image retention factor, 0.002, is well below the remedial level of 0.3.

The DQE is greatest for entrance air kermas in the range used by the AEC and above. At lower doses, electronic noise becomes significant and the DQE is lower.

The results of the optimisation study indicate that the beam qualities for different breast thicknesses selected under AEC control are close to optimal, and an increase in the tube load, particularly for the larger breasts, would enable the achievable level of image quality to be reached across the full range of breast thicknesses.

5.   CONCLUSIONS

The IMS Giotto 3DL system exceeded the minimum acceptable standard for image quality (for CNR) across all breast thicknesses, and the CDMAM results show image quality approaching the achievable level, except for the 0.1 mm details, at the dose levels achieved under AEC control. A 26% increase in image dose for an equivalent breast thickness of 60 mm would be needed to meet the achievable level of image quality for the 0.1 mm details. Adjustment of the doses under AEC control could enable the achievable level to be met for all thicknesses, whilst remaining within the dose limits.

REFERENCES

1. Workman A, Castellano I, Kulama E et al. *Commissioning and Routine Testing of Full Field Digital Mammography Systems* (NHSBSP Equipment Report 0604). Sheffield: NHS Cancer Screening Programmes, 2006.

2. Young KC, Johnson B, Bosmans H, et al. Development of minimum standards for image quality and dose in digital mammography. In *Digital Mammography* IWDM 2004, Proceedings of the Workshop in Durham NC, USA, June 2004, (2005).

3. Van Engen R, Young KC, Bosmans H, et al. The European protocol for the quality control of the physical and technical aspects of mammography screening. In: *European Guidelines for Quality Assurance in Breast Cancer Screening and Diagnosis*, 4th Edition, Luxembourg: European Commission, 2006.

4. Dance DR, Young KC, Van Engen RE. Further factors for the estimation of mean glandular dose using the United Kingdom, European and IAEA breast dosimetry protocols. *Physics in Medicine and Biology*, 2009, 54, 4361-4372.

5. Alsager A, Young KC, Oduko JM. Impact of Heel Effect and ROI Size on the Determination of Contrast-to-Noise Ratio for Digital Mammography Systems. In *Proceedings of SPIE Medical Imaging*, Bellingham WA: SPIE Publications, 2008, 69134: 1-11.

6. Young KC, Oduko JM, Bosmans H, et al. Optimal beam quality selection in digital mammography. *British Journal of Radiology*, 2006, 79: 981–990.

7. Young KC, Cook JJH, Oduko JM, et al. Comparison of software and human observers in reading images of the CDMAM test object to assess digital mammography systems. In *Proceedings of SPIE Medical Imaging,* Bellingham WA: SPIE Publications, 2006, 614206: 1–13.

8. Young KC, Cook JJH, Oduko JM. Automated and human determination of threshold contrast for digital mammography systems. In *Proceedings of the 8th International Workshop on Digital Mammography,* Berlin: Springer-Verlag, 2006, 4046: 266-272.

9. Young KC, Alsager A, Oduko JM et al. Evaluation of software for reading images of the CDMAM test object to assess digital mammography systems. In *Proceedings of SPIE Medical Imaging*, Bellingham WA: SPIE Publications, 2008, 69131C: 1-11.

10. *Determination of the detective quantum efficiency – Detectors used in mammography* (IEC 62220-1-2). Geneva: International Electrotechnical Commission, 2007.

11. Young KC, Cook JJH, Oduko JM. Use of the European protocol to optimise a digital mammography system. In *Proceedings of the 8th International Workshop on Digital Mammography,* Berlin: Springer-Verlag, 2006, 4046: 362–369.

12. Young KC, Oduko JM. *Technical Evaluation of Kodak DirectView Mammography Computerised Radiography System using EHR-M2 Plates* (NHSBSP Equipment Report 0706)*.* Sheffield: NHS Cancer Screening Programmes, 2007.

13. Young KC, Oduko JM. *Technical Evaluation of the Agfa CR-85 Mammography System* (NHSBSP Equipment Report 0707). Sheffield: NHS Cancer Screening Programmes, 2007.

14. Young KC, Oduko JM. *Technical Evaluation of the Hologic Selenia Full Field Digital Mammography System with a Tungsten Tube* (NHSBSP Equipment Report 0801)*.* Sheffield: NHS Cancer Screening Programmes, 2008.

15. Young KC, Oduko JM, Gundogdu O, et al. *Technical Evaluation of the GE Essential Full Field Digital Mammography System* (NHSBSP Equipment Report 0803). Sheffield: NHS Cancer Screening Programmes, 2008.

16. Oduko JM, Young KC, Alsager A, et al. *Technical Evaluation of the IMS Giotto Full Field Digital Mammography System with a Tungsten Tube* (NHSBSP Equipment Report 0804)*.* Sheffield: NHS Cancer Screening Programmes, 2008.

17. Young KC, Oduko JM, Alsager, A. *Technical Evaluation of the Sectra MDM-L30 Full Field Digital Mammography System* (NHSBSP Equipment Report 0805). Sheffield: NHS Cancer Screening Programmes, 2008.

18. Young KC, Oduko JM. Gundogdu O et al. *Technical Evaluation of the Konica Minolta Regius 190 CR Mammography System and Three Types of Image Plate* (NHSBSP Equipment Report 0806)*.* Sheffield: NHS Cancer Screening Programmes, 2008.

19. Young KC, Oduko JM. Gundogdu O. and Asad M. *Technical Evaluation of Profile Automatic Exposure Control Software on GE Essential Full Field Digital Mammography System* (NHSBSP Equipment Report 0903)*.* Sheffield: NHS Cancer Screening Programmes, 2009.

20. Young KC, Oduko JM, Asad M. *Technical Evaluation of Agfa DX-M Mammography CR Reader with HM5.0 Needle-IP* (NHSBSP Equipment Report 0905)*.*   Sheffield: NHS Cancer Screening Programmes, 2009.

21. Young KC, Oduko JM, Asad M. *Technical Evaluation of Fuji Amulet Full Field Digital Mammography System* (NHSBSP Equipment Report 0907)*.* Sheffield: NHS Cancer Screening Programmes, 2009.

22. Young KC, Oduko JM, Gundogdu O. and Alsager. *Technical Evaluation of Siemens Mammomat Inspiration Full Field Digital Mammography System* (NHSBSP Equipment Report 0909)*.*   Sheffield: NHS Cancer Screening Programmes, 2009.

23. Young KC, Oduko JM, Warren L. *Technical Evaluation of Hologic Selenia Dimensions 2-D Digital Breast Imaging System* (NHSBSP Equipment Report 1101). Sheffield: NHS Cancer Screening Programmes, 2011.